Dynamic synapses as archives of synaptic history: state-dependent redistribution of synaptic efficacy in the rat hippocampal CA1

Takuya Yasui, Shigeyoshi Fujisawa, Masako Tsukamoto, Norio Matsuki and Yuji Ikegaya

Laboratory of Chemical Pharmacology, Graduate School of Pharmaceutical Sciences, University of Tokyo, Tokyo 113-0033, Japan

Plastic modifications of synaptic strength are putative mechanisms underlying information processing in the brain, including memory storage, signal integration and filtering. Here we describe a dynamic interplay between short-term and long-term synaptic plasticity. At rat hippocampal CA1 synapses, induction of both long-term potentiation (LTP) and depression (LTD) was accompanied by changes in the profile of short-term plasticity, termed redistribution of synaptic efficacy (RSE). RSE was presynaptically expressed and associated in part with a persistent alteration in hyperpolarization-activated I_h channel activity. Already potentiated synapses were still capable of showing RSE in response to additional LTP-triggering stimulation. Strikingly, RSE took place even after reversal of LTP or LTD, that is, the same synapse can display different levels of short-term plasticity without changing synaptic efficacy for the initial spike in burst presynaptic firing, thereby modulating spike transmission in a firing rate-dependent manner. Thus, the history of long-term synaptic plasticity is registered in the form of short-term plasticity, and RSE extends the information storage capacity of a synapse and adds another dimension of functional complexity to neuronal operations.

(Resubmitted 13 March 2005; accepted after revision 20 April 2005; first published online 21 April 2005)
Corresponding author Y. Ikegaya: Laboratory of Chemical Pharmacology, Graduate School of Pharmaceutical Sciences, University of Tokyo, 7-3-1 Hongo, Bunkyo-ku, Tokyo 113-0033, Japan. Email: ikegaya@tk.air.jp

Neurones often have intrinsic membrane properties that generate complex spikes, sets of action potentials with narrow interspike intervals. Such spike barrages provoke use-dependent changes in synaptic responses of target neurones on a time scale of tens to hundreds of milliseconds, termed short-term plasticity (STP) (Zucker & Regehr, 2002). STP is believed to be of presynaptic origin and has several fundamental functions in signal processing, e.g. frequency-selective filtering of synaptic transmission (Varela *et al.* 1997; Fortune & Rose, 2001), detection of changes in presynaptic firing rates (Abbott *et al.* 1997), discrimination of temporal spike patterns (Buonomano & Merzenich, 1995), and stable coincidence detection (Cook *et al.* 2003). Cortical excitatory synapses usually exhibit a complex form of short-term facilitation and depression, and therefore, their responses to ongoing inputs are often complicated (Dobrunz & Stevens, 1997; Dobrunz & Stevens, 1999).

Recent work has indicated that at neocortical synapses, the profile of STP is shifted toward depression after induction of long-term potentiation (LTP), whereby the elevated synaptic efficacy almost disappears in later responses at higher frequencies of presynaptic firing (Markram & Tsodyks, 1996*a*). Such long-lasting changes in the profile of STP are called a redistribution of synaptic efficacy (RSE). At hippocampal synapses, however, RSE is unlikely to take place after LTP induction (Pananceau *et al.* 1998; Selig *et al.* 1999; Buonomano, 1999). Whether or not RSE exists is of functional importance because it leads to different interpretations of the role of LTP in neural processing. If LTP is not accompanied by RSE (as is the case at hippocampal synapses), neural information is evenly amplified at the synapses, i.e. a general gain increase of signals conveyed between neurones, whereas LTP with RSE (as is the case at neocortical synapses) transforms the 'content' of signals. Despite the intense efforts of several investigative groups, it still remains uncertain (or even controversial) whether RSE exists at all types of synapses or requires a specific protocol for its induction, whether RSE varies in amplitude and direction depending on the form of long-term plasticity, or what molecular mechanisms underlie RSE.

The present study shows that hippocampal synapses readily display RSE, but importantly, the incidence of RSE is determined by the properties of afferent stimuli used to induce long-term plasticity. Therefore, depending on patterns of synaptic inputs, LTP can transit between two distinct modes, i.e. gain-increase

DOI: 10.1113/jphysiol.2005.086595

and signal-rewriting modes. Moreover, we discover that depotentiation of LTP and dedepression of LTD are also accompanied by RSE although apparent synaptic strength, monitored by single-pulse stimulation, returns to baseline. Therefore, depotentiation/dedepression only ostensibly erases LTP/LTD, but depotentiated/dedepressed synapses still convey information about the past plasticity. These results might necessitate revision of the conventional assumptions regarding the function of synaptic plasticity. Finally, this work also reveals that RSE is expressed, at least in part, by a change of presynaptic I_h channel activity and may provide novel insights into the role of I_h channels in neural information processing.

Methods

Hippocampal slice preparations

Slices of hippocampi were prepared from 17- to 26-day-old Wistar/ST rats as previously described (Ueno *et al.* 2002), according to National Institutes of Health guidelines for laboratory animal care and safety. In brief, rats were decapitated after ether anaesthesia, and the brain was rapidly removed and put in ice-cold, modified artificial cerebrospinal fluid (aCSF) consisting of (mM): 124 NaCl, 25 $NaHCO_3$, 3 KCl, 1.24 KH_2PO_4, 1.4 $MgSO_4$, 2.2 $CaCl_2$, and 10 glucose, equilibrated with 95% O_2 and 5% CO_2. Transverse slices (400-μm thickness) were cut in chilled aCSF with a cooled ZERO-1 vibratome (DSK, Kyoto, Japan). After preincubation for at least 1 h in aCSF (32°C), slices were transferred to an interface recording chamber in which oxygenated aCSF (32°C) was continuously perfused. Incision was made between the CA2 and CA3 regions to prevent recurrent excitation before experiment.

Extracellular recordings

Bipolar tungsten electrodes (Frederick Haer & Co., Bowdoinham, ME, USA) were positioned on the CA1 stratum radiatum to stimulate the Schaffer collateral afferents; specifically the electrode was placed in the middle of a band of the stratum radiatum, i.e. at least 50 μm from either stratum pyramidale or lacunosum-moleculare and about 100 μm from the border between CA1 and CA2. A glass recording microelectrode filled with 0.15 M NaCl (~2 MΩ resistance) was also positioned in the centre of the CA1 stratum radiatum (about 200 μm from the stimulating electrodes). Test stimuli (50 μs duration) were delivered to the Schaffer collaterals every 30 s, and field EPSPs (fEPSPs) were recorded. The stimulus intensity was set to produce fEPSPs with half-maximal slopes, and all experiments were started after at least 30 min to ensure the stability of responses. In experiments using ZD7288, two stimulating electrodes were placed opposite the recording site, and single-pulse stimuli were delivered alternately every 15 s.

Whole-cell recordings

Whole-cell patch-clamp recordings from CA1 pyramidal cells were performed with borosilicate glass pipettes (4–8 MΩ) filled with intracellular solution containing (mM) 120 potassium gluconate, 20 KCl, 10 Hepes, 0.1 $CaCl_2$, 4 Mg-ATP and 0.2 EGTA (pH 7.4), as previously described (Tanaka *et al.* 1997). Recordings were carried out with an Axopatch 200B amplifier (Axon Instruments, Union City, CA, USA). Signals were low-pass-filtered at 1 kHz, digitalized at 10 kHz and analysed with pCLAMP 8.0 software (Axon Instruments). Neurones included for analysis had a resting potential lower than −50 mV, and fired overshooting action potentials in response to current injections. The stimulus intensity was set to produce EPSCs with half-maximal amplitude in Fig. 10 (voltage clamp mode) and EPSPs with about 80% of maximal amplitude in Fig. 11 (current clamp mode).

Estimation of mutual entropy

To estimate the fidelity of spike responses, we employed mutual entropy between presynaptic and postsynaptic firing patterns. All spike trains were transformed into strings consisting of '0s' and '1s' in successive 25-ms bins to construct a 'binary word', i.e. a vector in which '0' in a bin indicates the absence of a spike and '1' the occurrence of a spike. Each word consisted of 200 letters because our spike train template was 5000 ms in length (i.e. 5000/25 = 200). We then tabulated the probability of occurrence $p(W_i)$ of each word W_i and computed the associated entropy H, according to Shannon's formula:

$$H = -\sum_{W_i} p_n(W_i) \log_2 p_n(W_i)$$

The mutual information between the input spike train S_{in} and the output spike train S_{out} was estimated as follows:

$$H_{mutual}(S_{in}; S_{out}) = H(S_{out}) - H(S_{out}|S_{in})$$

in which $H(S_{out})$ is the entropy of postsynaptic spike trains, and $H(S_{out}|S_{in})$ is the conditional entropy, which is the entropy of postsynaptic spike trains given the presynaptic spike trains (Rieke *et al.* 1997; London *et al.* 2002). In order to evaluate the dependency of information transmission on the input frequency, we estimated the correlations between the mutual entropy and the firing rate of the presynaptic input. A cursor with a 1000-ms time window was slid along the time axis of a spike train to calculate the firing rate of presynaptic input for each time window and the mutual entropy between the presynaptic input and postsynaptic output spike trains. Then the mutual entropy was plotted *versus* the firing rate. Analyses were performed using a custom-written Igor routine (Wavemetrics, Lake Oswego, OR, USA).

Material

ZD7288 and CGP55845 were obtained from Tocris Cookson (Bristol, UK), and all other material was purchased from Sigma (St Louis, MO, USA). Drugs were dissolved in double-distilled water to make 100× stock solutions, except for 6-cyano-7-nitroquinoxoxaline-2,3-dione (CNQX), which was prepared in DMSO at 1000×. All stock solutions were stored at −20°C. They were diluted immediately before experiments. Drugs were bath applied, except for D,L-2-amino-5-phosphonopentanoic acid (AP5). AP5 was focally applied at a rate of ∼300 μl min^{-1} through a local perfusion pipette (280-μm i.d.) positioned ∼100 μm above the slice surface to block NMDA receptors on the spot.

We report the mean ± standard error of the mean for all measurements.

Results

RSE accompanies LTP at hippocampal synapses

The synapses exhibit various forms of STP in response to a sequence of presynaptic firing (Fig. 1). For instance, hippocampal mossy fibre–CA3 synapses and climbing fibre–Purkinje cell synapses display prominent short-term facilitation, whereas parallel fibre–Purkinje cell synapses show depression. At most synapses including Schaffer collateral–CA1 synapses, however, short-term facilitation and depression coexist, and the profile of STP is complex and often dynamic.

In order to quantify STP, we measured the STP ratio, defined here as a percentage of each response ($fEPSP_N$) to the first response ($fEPSP_1$) in a burst train (Fig. 1). Thus, STP ratios are higher than 100% at facilitating synapses (Fig. 1*A* and *D*) and lower than 100% at depressing synapses (Fig. 1*C* and *D*). At complex synapses like Schaffer collateral–CA1 synapses, the STP ratios are usually higher than 100% in fEPSP2 and become lower in later responses. The STP ratio usually reaches a steady state in fEPSP8–10 in a train (see below), and therefore we referred to the mean STP ratio of fEPSP8–10 simply as a 'STP ratio' unless otherwise specified.

In rat hippocampal slices, we monitored STP at Schaffer collateral–CA1 synapses by applying a brief train (10 pulses) at 40 Hz every 5 min in the presence of 50 μM D,L-AP5 to prevent induction of NMDA receptor-dependent plasticity. This frequency (40 Hz) corresponds to gamma oscillations, which are often observed in the hippocampus *in vivo* (Csicsvari *et al.* 2003). Because AP5 is present, the gamma-frequency burst trains did not induce a persistent change in fEPSPs evoked by single-pulse stimulation (or $fEPSP_1$) (Fig. 2*A* and *C*, time −30 to 0 min). Under these control conditions, 10 successive fEPSPs evoked by a 10-pulse train, i.e. $fEPSP_1$∼$fEPSP_{10}$, were not identical in their slopes; $fEPSP_2$ was larger than the $fEPSP_1$ whereas later fEPSPs were rather suppressed (Fig. 2*A*). The mean percentage of $fEPSP_{8–10}$ to $fEPSP_1$ slopes, i.e. the STP ratio, was 85.3 ± 2.8% ($n = 22$ slices). Thus, CA1 synapses are depressing in the late, steady-state phase of a burst response.

To examine how the induction of LTP affects STP, we tetanized the Schaffer collaterals at 100 Hz (100 pulses) 15 min after AP5 washout, and immediately the slices were reperfused with AP5 to test the same gamma trains as before. The 100-Hz tetanus induced robust LTP of $fEPSP_1$, and this LTP was maintained for > 150 min of our observation period (Fig. 2*A*). Thirty seconds after LTP induction, the responses to a 10-pulse train

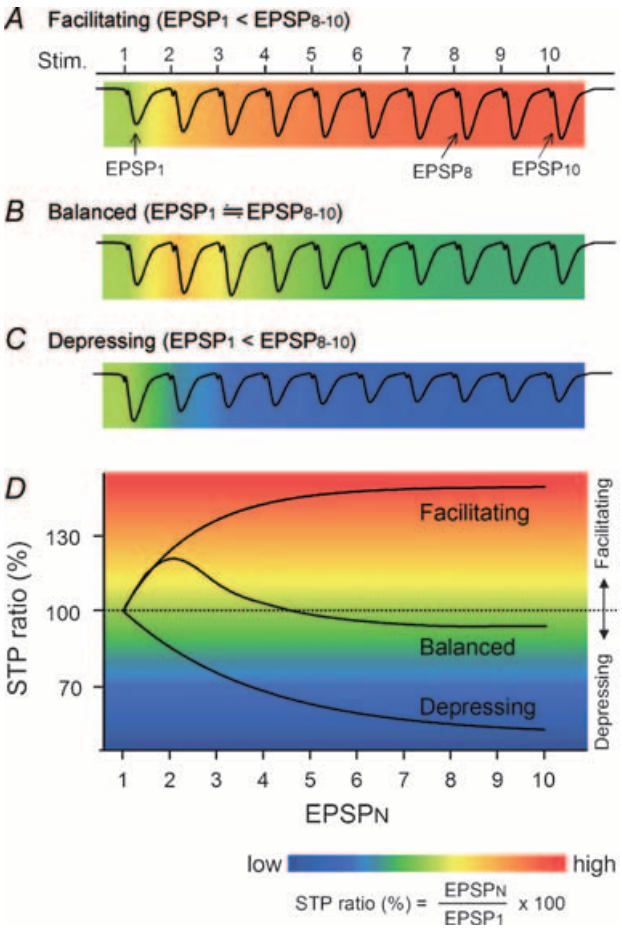

Figure 1. Schematic drawing of various types of STP
A–C, each wave represents a synaptic response to a 10-pulse train at 40 Hz and is merged with a pseudocolour-scale image of STP ratios, which are calculated from the equation indicated below panel *D*. Based on the mean STP ratio of $EPSP_{8–10}$, synapses are classified into facilitating (*A*), balanced (*B*) or depressing synapses (*C*). *D*, the relationship of three synaptic states. The STP ratio usually becomes stationary for the 8th–10th pulses in a train, and therefore, unless otherwise specified, we referred to the STP ratio of $EPSP_{8–10}$ simply as 'STP ratio'. RSE is defined as a change in the STP ratio after induction of synaptic plasticity.

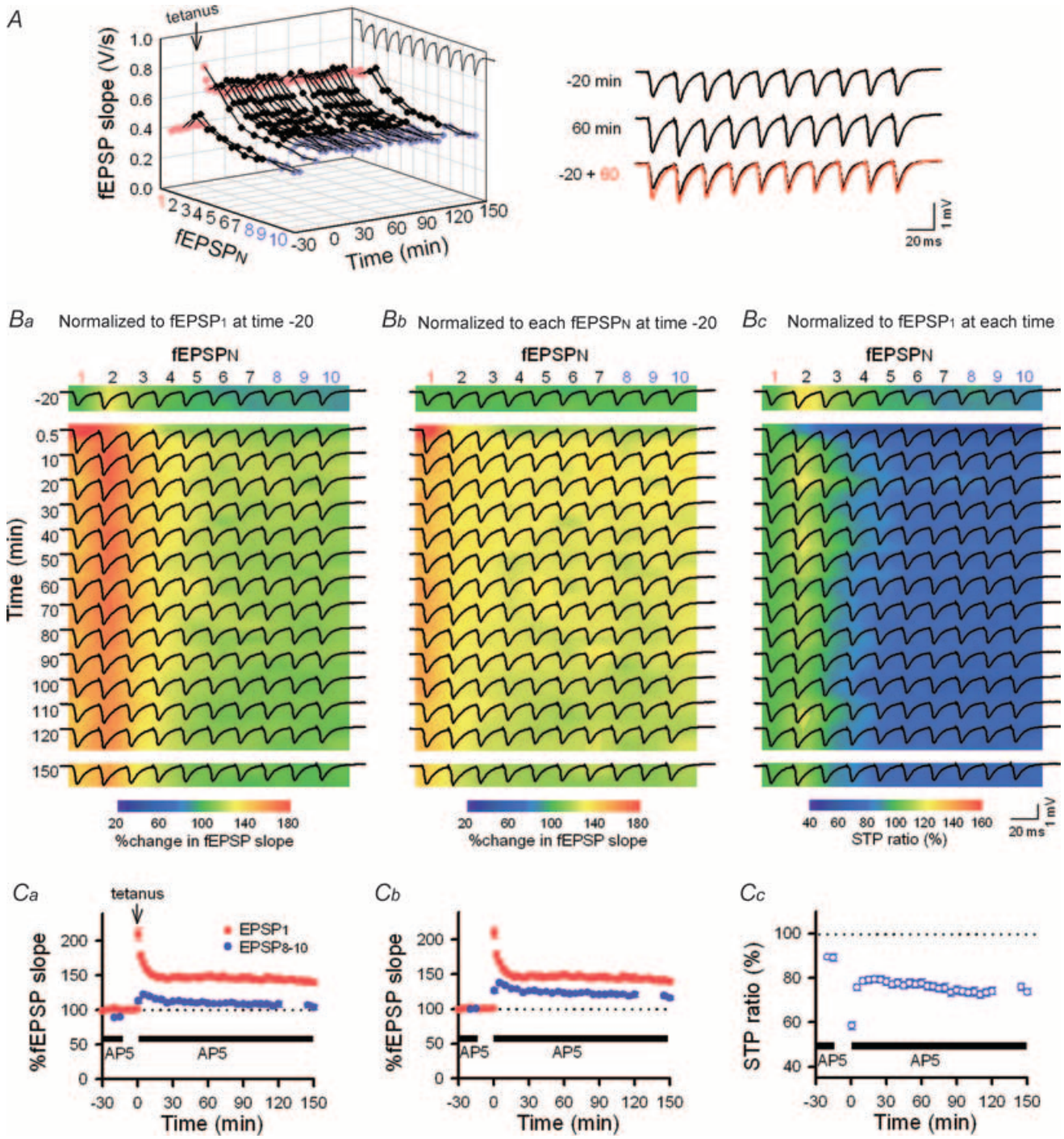

Figure 2. Changes in the STP profiles (i.e. RSE) induced by LTP induction at Schaffer–CA1 synapses
A, time course of LTP monitored by single-pulse stimuli (every 30 s, red). LTP was induced by tetanic stimulation (100 pulses at 100 Hz) at time 0 min and maintained over 150 min. To monitor the response to burst firing, 10-pulse trains at 40-Hz were applied at times −20, −15, 145 and 150 min and every 5 min during time 0.5–120 min. AP5 was absent during the period from time −15 to 0 min. The right panels show burst responses at time −20 and 60 min. Note that the degree of potentiation was smaller in later responses in a burst (fEPSP8–10, blue) as compared to the initial response ($fEPSP_1$), which is indicative of RSE. *B*, traces of synaptic responses (the same data as the panel *A*) are superimposed onto the pseudocoloured images that show ratios of individual fEPSPs to $fEPSP_1$ at time −20 min (*Ba*), to the corresponding $fEPSP_N$ at time −20 min (*Bb*), and to $fEPSP_1$ at each time point, i.e. the STP ratio (*Bc*). *C*, average data for each parameter in the panel *Ba–c* ($n = 8$ slices). The degree of a change in $fEPSP_{8–10}$ was smaller than that seen in $fEPSP_1$, that is, the STP ratio was reduced after LTP induction. This change was maintained over 150 min.

were entirely potentiated, but to a different extent in individual fEPSPs, that is, fEPSP1 was augmented more prominently than $fEPSP_{8–10}$, with the STP ratio equal to $43.7 \pm 2.9\%$ in consequence. During the following trains, these post-tetanic changes were gradually abated to a stationary state; 30 min after tetanus, $fEPSP_1$ was stabilized at $144.2 \pm 3.6\%$ relative to the level before potentiation, but $fEPSP_{8–10}$ at only $125.9 \pm 2.8\%$ ($n = 8$ slices) (Fig. 2*A* and *Cb*). For better understanding, we showed the same data in three different ways (Fig. 2*B* and *C*); individual $fEPSP_N$ slopes were normalized to the baseline $fEPSP_1$ slope at −20 min prior to tetanus (Fig. 2*Ba* and *Ca*), to the corresponding $fEPSP_N$ slopes at time −20 (Fig. 2*Bb* and *Cb*), and to the $fEPSP_1$ slope at each time point (i.e. STP ratios, Fig. 2*Bc* and *Cc*). Among these representations, the STP ratios in Fig. 2*Bc* and *Cc* seem to be the most appropriate for evaluating synaptic states, i.e. short-term facilitation or depression. We therefore adopted this measurement in the following experiments. The LTP induction significantly reduced the STP ratio to $74.4 \pm 3.7\%$, which corresponded with a $15.2 \pm 1.7\%$ reduction in STP ratio from the pretetanus level ($P < 0.01$, Fig. 2*Cc*). Similar results were obtained by measuring fEPSP amplitudes (instead of their slopes): 30 min after LTP induction, $138.2 \pm 4.2\%$ for $fEPSP_1$ amplitude and $75.5 \pm 2.4\%$ for STP ratio (a $14.2 \pm 2.2\%$ reduction) relative to the pretetanus baseline. These results are indicative of RSE; note that RSE was defined here as a change in the STP ratio (ΔSTP ratio) following the induction of long-lasting synaptic plasticity.

Based on its molecular mechanisms, the state of LTP is classified into different stages, e.g. kinase dependent, protein synthesis dependent, and gene transcription dependent phases (Bliss & Collingridge, 1993). Nonetheless, the degree of RSE as well as potentiated $fEPSP_1$ was kept almost constant for up to 150 min (Fig. 2*A*, *Cb* and *Cc*). RSE was unchanged even after a 25-min idle period, during which no burst train was applied (Fig. 2*A*, *Bc* and *Cc*). Therefore, RSE is unlikely to be due to an artifact of gamma-frequency trains applied every 5 min to monitor STP responses.

To determine whether RSE takes place under more physiological conditions, we repeated the same series of experiments in the absence of AP5 (Fig. 3*A*). $fEPSP_1$ and STP ratio were both stable in the presence of AP5, but after AP5 washout, application of burst trains elicited a gradual increase in $fEPSP_1$. At the same time, later fEPSPs in the trains also exhibited gradual potentiation, but to a smaller degree than $fEPSP_1$ (Fig. 3*A*), which resulted in RSE that resembled tetanus-induced RSE (Fig. 3*B*). The increased $fEPSP_1$ and late fEPSPs were stabilized after three or four burst trains. Again, the established RSE was unchanged after a 30-min idle period during which trains were absent (Fig. 3*B*). Thus, RSE is inducible under more physiological conditions.

Bidirectional synaptic plasticity is linked to bidirectional RSE

We next examined whether RSE accompanies long-term depression (LTD), another form of long-lasting synaptic plasticity. Low-frequency stimulation (LFS, 900 pulses at 1 Hz) was used to induce LTD. LFS depressed all initial fEPSPs in the following trains, but changed later fEPSPs in the train to a different extent; $fEPSP_1$ was decreased to $71.7 \pm 4.3\%$, and $fEPSP_{8–10}$ to $83.2 \pm 4.5\%$ relative to the baseline level, resulting in $101.6 \pm 3.5\%$ of STP ratio, which corresponded with an $18.9 \pm 2.8\%$ increase

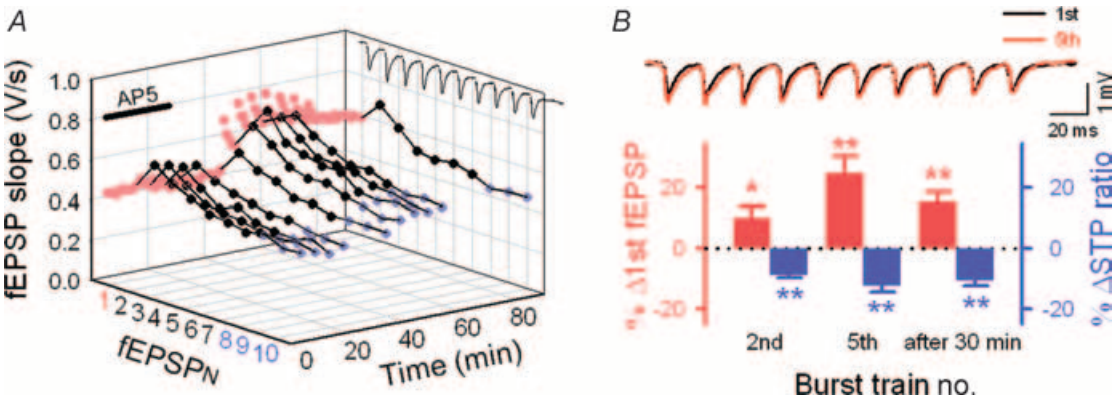

Figure 3. Spontaneously occurring RSE in the absence of AP5
A, in the presence of AP5, the responses to the bursts were stable, but after AP5 washout at time 30 min, $fEPSP_1$ exhibited gradual augmentation along application of the burst trains every 5 min (5 times), in which case the degrees of potentiation were smaller in later fEPSPs than $fEPSP_1$, that is, 10-pulse trains at 40 Hz alone induced RSE similar to that induced by LTP. RSE was preserved even after a 30-min period during which burst trains were absent. *B*, summary of STP changes spontaneously occurring in the absence of AP5. The top panel indicates synaptic responses evoked by the first (i.e. basal response, black) and fifth (red) application of burst trains. The bottom graph shows changes in fEPSP1 and STP ratio from the basal response as a percentage. $^*P < 0.05$, $^{**}P < 0.01$ *versus* basal response; Tukey's test after ANOVA (n = 5–8 slices).

in STP ratios (after 30 min, $P < 0.01$, $n = 7$ slices) (Fig. 4*A* and *C*). This modification is opposite to the direction of LTP-induced RSE. As a result, synapses with LTD were no longer depressing on a short time scale, even facilitating in some cases (Fig. 4*A*). We therefore conclude that RSE enables synapses to transit between facilitating and depressing.

The direction and degree of long-term plasticity depend on the intensity of synaptic activation during induction. Experimentally, varying levels of synaptic plasticity, i.e. a continuum from LTD to LTP, can be induced by changing the number and frequency of afferent stimulations. To determine whether different levels of synaptic plasticity are associated with different levels of RSE, we applied diverse

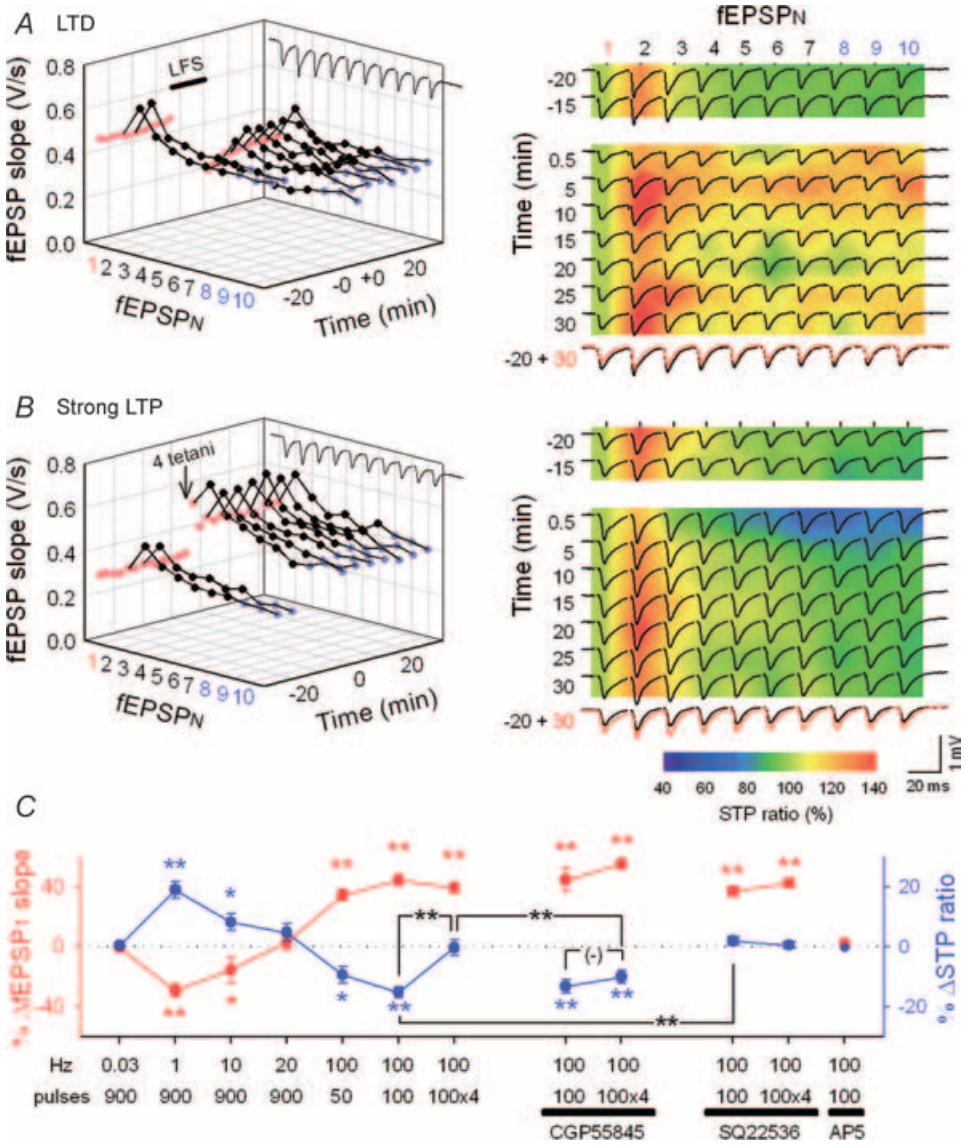

Figure 4. Activity-dependent, bidirectional RSE
A and *B*, representative STP changes induced by 900 pulses at 1 Hz (*A*), or four 100 pulses at 100 Hz (*B*). Time courses of fEPSP slopes are plotted in the left panels. The right panels indicate 10 fEPSP slopes normalized to $fEPSP_1$ in each train on a pseudocolour scale, on which raw field responses were superimposed. The bottom-right panels merge two traces 20 min before and 30 min after LFS or tetanus. *D*, summary of bidirectional synaptic plasticity and RSE. Changes in $fEPSP_1$ (red) displayed a BCM-like sigmoid curve (Bienenstock *et al.* 1982), and they were correlated inversely with the mean changes in fEPSP8–10 relative to $fEPSP_1$ in each train (ΔSTP ratio, blue), except for four tetani (100 pulses at 100 Hz), which did not alter the STP ratio. In the presence of 1 μM CGP55845, however, four tetani decreased the STP ratio to a degree similar to that after one tetanus-induced LTP. In contrast, one tetanus-induced RSE was blocked by 100 μM SQ22536. AP5 blocked the induction of both LTP and RSE. Data were obtained 15 min before and 30 min after tetanus. $^*P < 0.05$, $^{**}P < 0.01$ *versus* basal response; Tukey's test ($n = 5$–8 slices).

patterns of repetitive stimulation, i.e. 900 pulses at 0.03 Hz, 900 pulses at 10 Hz, 900 pulses at 20 Hz, and 50 pulses at 100 Hz. These conditions of stimulation induced various levels of LTP or LTD and depicted an activity–response curve of long-term plasticity of $fEPSP_1$ (Fig. 4*C*, red). Changes in STP ratios (i.e. RSE) were roughly inversely correlated with the $fEPSP_1$ changes (Fig. 4*C*, blue).

When AP5 was present during tetanus or LFS, neither LTP/LTD nor RSE could occur ($n = 3$–4 each, data not shown, but for LTP, see Fig. 4*C*). The data indicate that the induction of RSE is NMDA receptor dependent, probably requiring the induction of long-term plasticity.

Under our experimental conditions, fEPSPs monitored by single-pulse stimulation ($fEPSP_1$) expressed $144.2 \pm 3.6\%$ upon LTP induced by 100 pulses at 100 Hz (after 30 min, $n = 8$ slices), and an additional three sequential tetani, applied at an interval of 30 s, brought the level of potentiation to $139.0 \pm 3.6\%$ from baseline, not significantly different from the level when one tetanus was delivered ($P > 0.1$, $n = 7$ slices) (Fig. 4*B* and *C*). In spite of showing the almost same $fEPSP_1$ changes, synapses exposed to one and four tetani had different STP ratios. After four tetani, the $fEPSP_{8–10}$ was potentiated to $137.0 \pm 4.7\%$, which was nearly equal to the level of potentiation of $fEPSP_1$. Thus, the STP ratio was $85.5 \pm 6.5\%$, and this value was almost equal to the pretetanus level and significantly larger than that induced by one tetanus (Fig. 4*B* and *C*). These data suggest that potentiated synapses are still capable of displaying further plasticity in the form of RSE in response to LTP-triggering stimulation. This may explain the apparent inconsistency between studies showing that RSE is present at neocortical synapses (Markram & Tsodyks, 1996*a*; Buonomano, 1999) but not at hippocampal synapses (Pananceau *et al.* 1998; Selig *et al.* 1999; Buonomano, 1999). Our observations indicate that whether or not RSE accompanies LTP is determined by the intensity of synaptic activation. In other words, RSE is induced by weak, but not strong, afferent stimulation.

$GABA_B$ receptor activation prevents the induction of RSE

What is the mechanism responsible for the difference in STP between one and four tetani? We focused on GABAergic transmission because GABA release from inhibitory interneurones is increased over an hour after repetitive stimulation (Perez *et al.* 1999; Caillard *et al.* 1999), and presynaptic $GABA_B$ receptors on excitatory neurones may affect STP by regulating transmitter release (Gerber & Gahwiler, 1994; Brenowitz *et al.* 1998). To block the activity of $GABA_B$ receptors, slices were continuously perfused with 1 μM CGP55845, a specific $GABA_B$ receptor antagonist. CGP55845 did not influence STP ratios during the control period (STP ratio: $82.5 \pm 5.3\%$ in CGP55845, $n = 14$) or RSE induced by one tetanus (Fig. 4*C*). However, in the presence of CGP55845, four tetani readily induced RSE (Fig. 4*C*); the RSE degree was no longer different between one and four tetani in the presence of CGP55845 ($P > 0.1$, Fig. 4*C*). Therefore, under normal conditions, strong synaptic activation, i.e. four tetani, recruits $GABA_B$ receptors, which may inhibit the induction of RSE.

Another candidate molecule that may regulate RSE is cAMP. It is reported that cAMP increased by brief application of forskolin, an adenylyl cyclase activator, induces LTP-like potentiation and an alteration in STP at Schaffer collateral–CA1 synapses (Lu & Gean, 1999). It is possible therefore that cAMP mediates the induction of RSE. To block the action of cAMP, experiments were carried out in the presence of 100 μM SQ22536, an adenylyl cyclase inhibitor. SQ22536 abolished RSE induced by one tetanus (Fig. 4*C*), whereas it did not influence the STP ratios of baseline (STP ratio: $90.0 \pm 3.9\%$ in SQ22536, $n = 8$) or after four tetani (Fig. 4*C*). Therefore, cAMP is required for the RSE induction. Given that activation of $GABA_B$ receptors causes a decrease in cAMP via the G_o/G_i class of G proteins (Misgeld *et al.* 1995), it is plausible that strong synaptic inputs (e.g. four tetani) activate $GABA_B$ receptors in presynaptic terminals and reduce the cAMP levels, thereby preventing the induction of RSE.

RSE represents the state of synapses

LTP is believed to disappear when appropriately patterned activity arrives at synapses in the immediate aftermath of potentiation. This phenomenon is termed depotentiation (Fujii *et al.* 1991; Staubli & Scafidi, 1999; Huang *et al.* 2001). No study has yet examined whether RSE disappears together with depotentiation. When LFS (900 pulses at 1 Hz) was delivered 5 min after one tetanus (100 pulses at 100 Hz), the once potentiated $fEPSP_1$ was reduced to the pretetanus level, i.e. depotentiation ($98.1 \pm 2.2\%$ of control, $n = 8$ slices). Interestingly, however, later fEPSPs in a burst train remained potentiated; 30 min after depotentiation, the $fEPSP_{8–10}$ slopes still stayed at $111.1 \pm 3.0\%$ relative to baseline (Fig. 5*A*). After depotentiation, therefore, the STP ratio was increased to $102.6 \pm 3.7\%$, which was significantly higher than $86.7 \pm 2.5\%$ of the pre-LTP baseline ($P < 0.01$) (Fig. 5*A* and *D*). These results indicate that depotentiation does not completely reverse synaptic efficacy to the pretetanus state.

Likewise, reversal of LTD (dedepression) (Dudek & Bear, 1993; Lee *et al.* 2000), which was attained by a weak tetanus (50 pulses at 100 Hz) 5 min after LTD induction, also restored only $fEPSP_1$ in a burst (Fig. 5*B* and *D*). In this case, the LTD-reversing protocol augmented later fEPSPs to a larger extent than $fEPSP_1$ and increased the STP ratio to $101.9 \pm 1.4\%$, significantly larger than $86.9 \pm 4.2\%$ of the pre-LTD baseline (Fig. 5*B* and *D*). This suggests that RSE

provides depotentiated and dedepressed synapses with unique functional states that differ from naive states, LTP, or LTD.

To further confirm this, we carried out 'normalization' of LTP, in which we reduced the intensity of test stimuli 30 min after plasticity induction and adjusted $fEPSP_1$ slopes to baseline. The normalization procedures preserved the level of LTP-induced RSE (Fig. 5*C*), and therefore, the state of the normalized synapses was different from that of depotentiated synapses.

Various forms of synaptic plasticity and their RSE are summarized in Fig. 5*D*. Different synaptic states were plotted at different points in the space of changes in $fEPSP_1$ and STP ratios, except for the relationship between depotentiation and dedepression. This indicates that the history of synaptic activity can be encoded into the forms of $fEPSP_1$ and STP.

Under physiological conditions, the rhythm of synaptic inputs is not limited to the gamma-range frequency. The profile of STP is known to vary with presynaptic firing rate

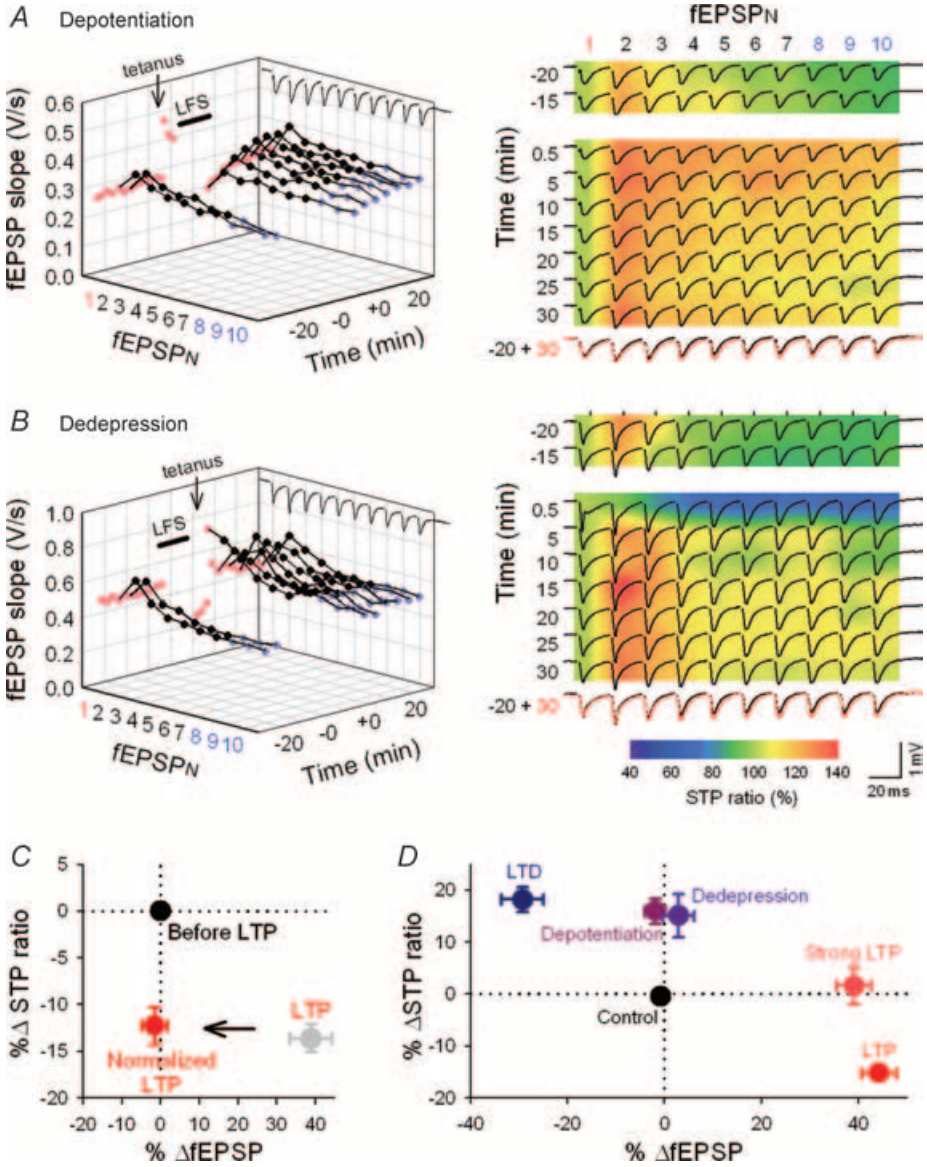

Figure 5. Synaptic states are discriminated by RSE
A–B, representative RSE after depotentiation (*A*) and dedepression (*B*). *A*, depotentiation was induced by LFS (900 pulses at 1 Hz) applied 5 min after tetanus (100 pulses at 100 Hz). Only $fEPSP_1$ was returned to the baseline level, but later fEPSPs were kept augmented after depotentiation. The right panels merged raw traces with pseudocolour images of STP ratios (for details, see Fig. 3 legend). *B*, weak tetanus (50 pulses at 100 Hz) 5 min after low-frequency stimulation was given to induce dedepression. Again, only $fEPSP_1$ was returned to baseline. *C*, artificially normalized LTP preserves the level of RSE. Potentiated synaptic responses (grey) were adjusted to pretetanus baseline by reducing the intensity of test stimulation. Even though $fEPSP_1$ returned to the pretetanus level, synapses preserve the level of RSE. $n = 8$ slices. *D*, summary of RSE induced by various types of long-term plasticity.

(Dittman *et al.* 2000). It is possible that RSE is also changed as a function of input frequency. We therefore tested burst trains at frequencies ranging from 1 to 50 Hz (Fig. 6*A*–*C*). STP was not observed at 1 Hz of burst frequency. As the frequency was increased, both STP and RSE became evident in all cases of LTP, LTD and depotentiation (Fig. 6*A*–*C*). Data are summarized in Fig. 6*D*. RSE was more apparent at higher rates of presynaptic firing, but the direction of RSE was unchanged across frequencies. Therefore, the direction of RSE is determined by synaptic states, but not by input frequency. We were unable to perform precise analysis for RSE at frequencies higher than 50 Hz because neighbouring fEPSPs overlapped with one other.

Presynaptic I_h mediates the maintenance of RSE

To identify the synaptic origin of STP at hippocampal synapses, we compared the STP ratios before and after treatment with 0.1 μM CNQX, a competitive antagonist

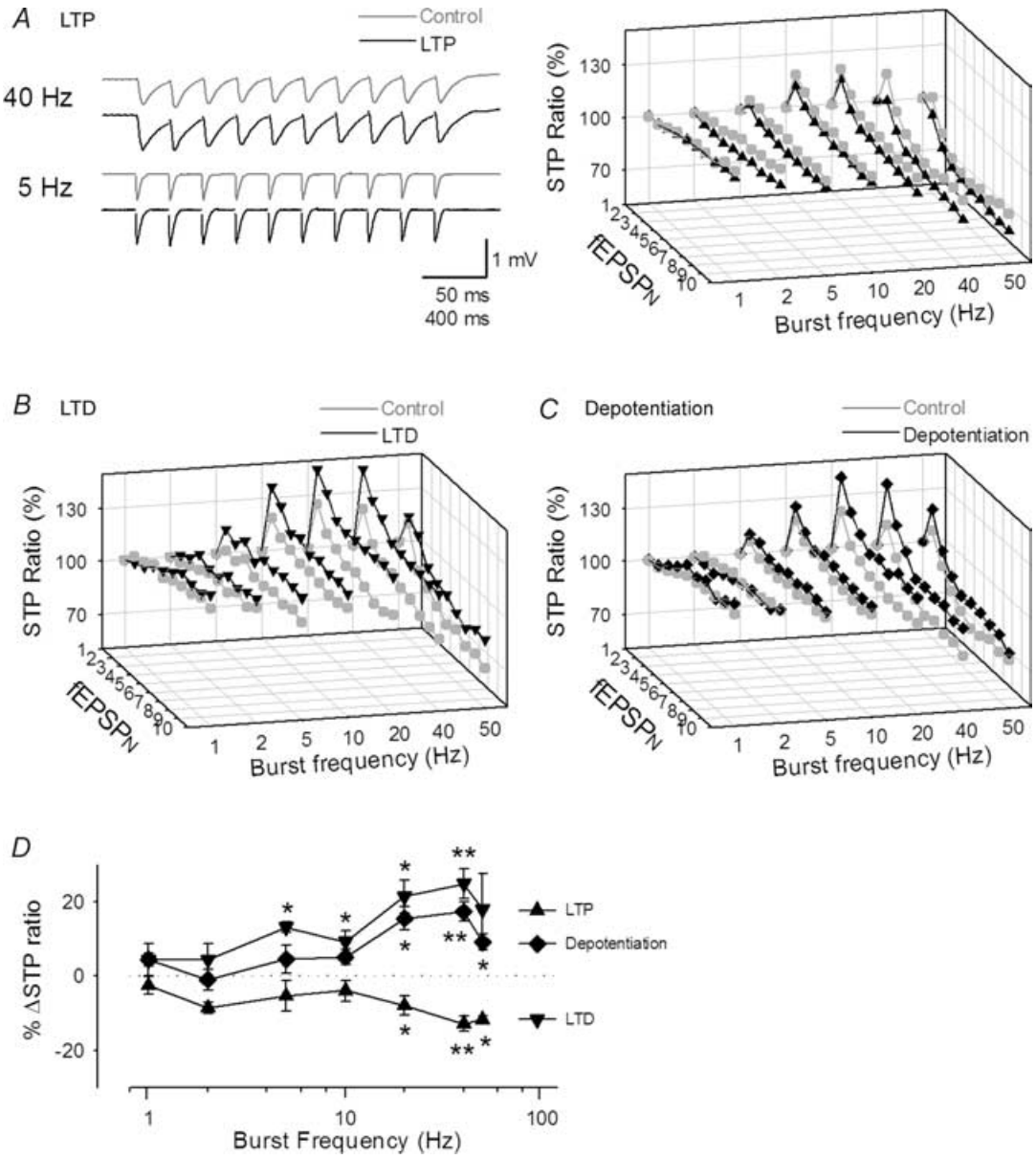

Figure 6. Input-frequency dependence of RSE
A–*C*, representative STP evoked by burst trains with various frequencies of inputs before (Control) and after induction of LTP (*A*), LTD (*B*) and depotentiation (*C*). LTP and LTD were induced by stimulation consisting of 100 pulses at 100 Hz and 900 pulses at 1 Hz, respectively. Depotentiation was induced by applying LFS 5 min after tetanus of 100 pulses at 100 Hz. Data were obtained 15 min before and 30 min after plasticity induction. RSE was more evident at higher input frequency, but the direction of RSE was presented across frequencies. *D*, summary of the frequency dependence of RSE. $^*P < 0.05$, $^{**}P < 0.01$ *versus* basal response; Tukey's test ($n = 4$ slices).

of non-NMDA receptors. At this low dose, CNQX partially blocks synaptic transmission, reducing the postsynaptic sensitivity to glutamate (Varela *et al.* 1997). Under these conditions, CNQX attenuated individual fEPSPs throughout a burst to approximately the same extent, retaining the STP ratio (Fig. 7*A*). Therefore, the postsynaptic modification does not affect the profile of STP.

We next modified external Ca^{2+} concentrations ($[Ca^{2+}]_o$), a procedure known to alter the probability of transmitter release from presynaptic terminals. This manipulation induced dramatic changes in STP as well as $fEPSP_1$; lowering $[Ca^{2+}]_o$ from 2.2 mM to 1.2 mM resulted in a decrease in $fEPSP_1$ and an increase in STP ratios, an effect that resembles LTD-induced RSE (Fig. 7*B*), whereas raising $[Ca^{2+}]_o$ from 2.2 mM to 4 mM increased $fEPSP_1$ and decreased STP ratios, resembling LTP-induced RSE (Fig. 7*C*). Data are summarized in Fig. 7*D*. These results are consistent with the consensus that STP is presynaptically expressed through a change in release probability (Markram & Tsodyks, 1996*b*; Tsodyks & Markram, 1997; Abbott & Nelson, 2000).

Accumulating evidence indicates that hyperpolarization-activated cation current (I_h) channels are highly expressed in hippocampal pyramidal cells (Santoro *et al.* 2000) and that presynaptic I_h modulates synaptic transmission in the hippocampus (Mellor *et al.* 2002) and the cerebellum (Southan *et al.* 2000). Soleng *et al.* (2003, 2004) suggested that I_h channels affect the synaptic release machinery at hippocampal CA3 axons. Furthermore, I_h channels are known to undergo a modulation by cAMP (Pape, 1996; Abi-Gerges *et al.* 2000), and cAMP is likely to mediate RSE (Fig. 4*C*). We thus investigated the possible involvement of I_h in RSE. Under control conditions, ZD7288, an I_h channel inhibitor (Harris & Constanti, 1995), reduced the STP ratio from $85.7 \pm 3.5\%$ to $72.1 \pm 3.0\%$ ($P < 0.01$, $n = 6$ slices), with a slight increase in $fEPSP_1$ slopes by $9.2 \pm 1.8\%$ (Fig. 8*A*).

To determine whether ZD7288 acts at presynaptic or postsynaptic sites, we carried out patch-clamp recordings from CA1 pyramidal cells. Postsynaptic I_h was elicited by hyperpolarizing voltage steps from −60 mV, emerging as a slow inward current that was inhibited by bath application

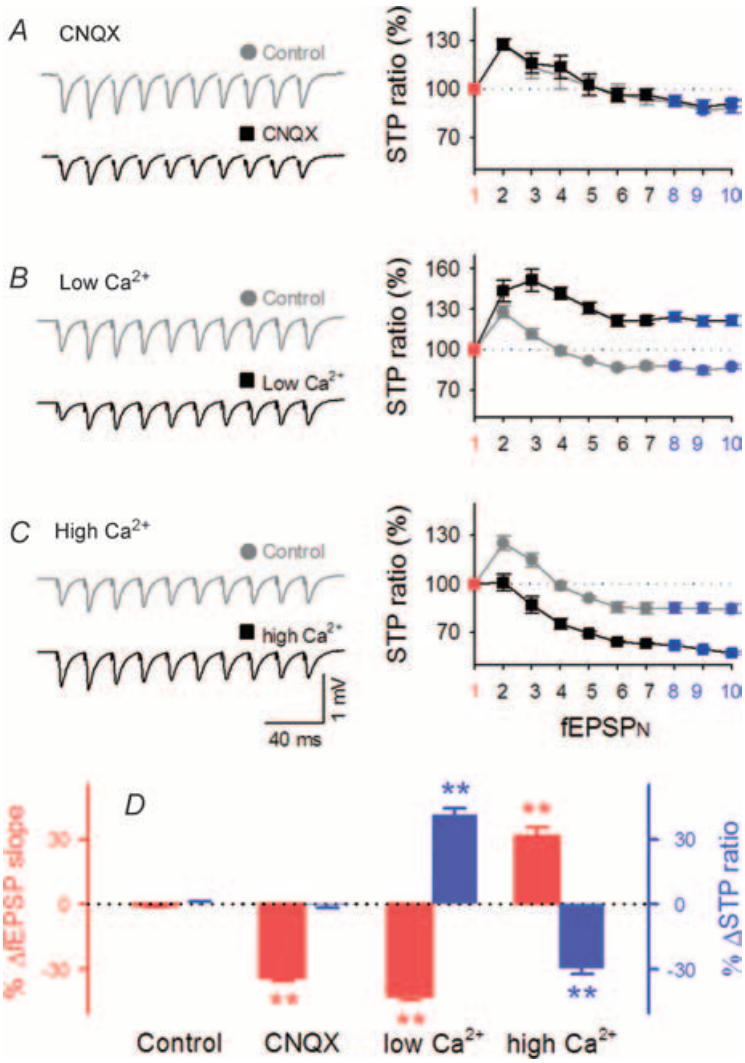

Figure 7. STP has presynaptic origins
A–C, effects of low-dose CNQX (*A*), and low (*B*) and high concentrations of external Ca^{2+} (*C*) on 10 fEPSPs evoked by 40-Hz trains. Left traces are typical field recordings. Right panels show responses relative to $fEPSP_1$ (STP ratios) in each train. *D*, summarized data of panels *A–C*. $^*P < 0.05$, $^{**}P < 0.01$ *versus* control response; Tukey's test ($n = 4$–7 slices).

of 30 μM ZD7288 (Fig. 9*Aa*). When a postsynaptic cell was intracellularly loaded with 100 μM ZD7288 through the patch pipette, the step pulse-induced inward currents displayed no apparent slow component or were not affected by further bath application of ZD7288 (Fig. 9*Ab*). Thus, intracellular application of ZD7288 selectively abolishes postsynaptic I_h and allows us to discriminate the postsynaptic contributions of I_h from presynapic I_h.

The postsynaptic I_h is reported to suppress dendritic integration of excitatory inputs in CA1 pyramids (Magee, 1998, 1999). Consistent with this, the extracellular application of ZD7288 enhanced temporal EPSC summation during a 40-Hz train, resulting in an increase of the STP ratio (Fig. 9*Ba* and *C*). This effect is different from that seen in field potential recordings (see Fig. 8*A*) and probably due to dendritic I_h in postsynaptic neurones because such prominent EPSC accumulation was not observed when cells was intracellularly loaded with ZD7288 (Fig. 9*Bb* and *C*). In ZD7288-loaded cells, extracellular application of ZD7288 induced a slight increase in EPSC1 and a decrease in the STP ratio (Fig. 9*Bb* and *C*). This effect is now similar to that seen

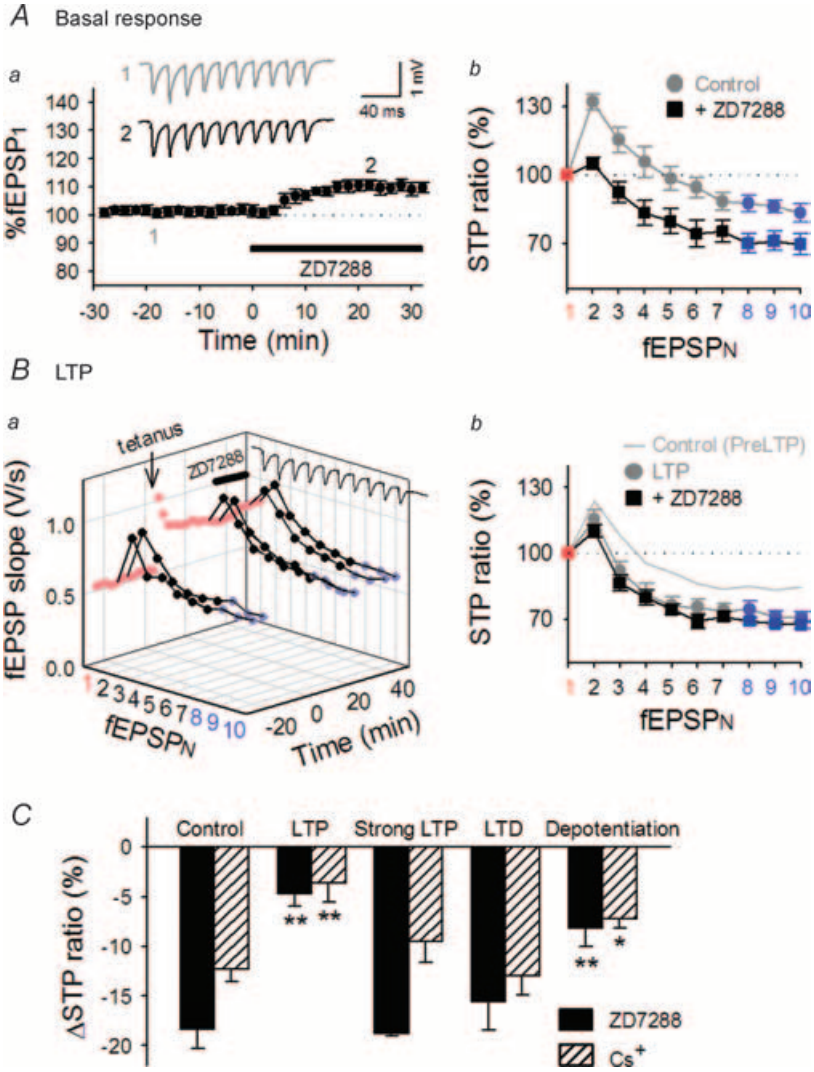

Figure 8. I_h activity contributes to the expression of RSE
A, effect of 30 μM ZD7288, an I_h channel blocker, on STP under basal conditions. *Aa*, the time course of changes in $fEPSP_1$ slopes following ZD7288 perfusion. Representative recordings at time −20 and 20 are shown in the inset. *Ab*, the STP ratio of 10 successive fEPSPs, which were normalized to each $fEPSP_1$. *B*, effect of 30 μM ZD7288 on STP after LTP induction. *Ba*, the time course of changes in fEPSPs slopes following ZD7288 perfusion 30 min after tetanus (100 Hz, 100 pulses). *Bb*, the STP ratio was reduced after LTP induction, and no additional decrease in STP ratios was induced by application of ZD7288, that is, the effects of LTP and ZD7288 on STP were occlusive. *C*, comparisons of the effects of ZD7288 and Cs^+ before and after various synaptic experiences. The same protocol as shown in panel *B* was used. ZD7288 and Cs^+ became ineffective at synapses that experienced LTP and depotentiation, but not LTD or strong LTP. $^*P < 0.05$, $^{**}P < 0.01$ *versus* control; Tukey's test ($n = 5$–7 slices).

in field potential recordings (see Fig. 8*A*). Therefore, the results of field recordings mainly reflected the presynaptic effect of ZD7288; note that field recordings monitor synaptic transmission directly in the stratum radiatum, a synapse-rich area, whereas in whole-cell recordings, synaptic transmission is subject to contamination of post-synaptic dendritic processing. We therefore conclude that ZD7288-decreased STP ratios, seen in Fig. 8*A* and 9*Bb*, are attributable to inhibition of presynaptic I_h.

We sought to determine whether I_h contributes to RSE. If the I_h activity is involved in RSE expression, the sensitivity of STP to ZD7288 is expected to change after the induction of long-term plasticity. After LTP induction, ZD7288 application caused a similar increase in $fEPSP_1$ to $107.2 \pm 2.2\%$ (Fig. 8*B*), which indicates that LTP did not occlude the ZD7288 effect on $fEPSP_1$. Strikingly, however, ZD7288 did not reduce the STP ratios at these potentiated synapses (Fig. 8*B*). Similar results were obtained at depotentiated synapses (Fig. 8*C*). These results indicate that I_h does not contribute to STP at potentiated or depotentiated synapses. RSE is hence likely to be expressed by a decrease in presynaptic I_h activity. In contrast, a ZD7288-induced decrease in the STP ratios was normally observed after strong LTP and LTD (Fig. 8*C*).

In all the above experiments with ZD7288, we used two independent stimulating electrodes and carefully

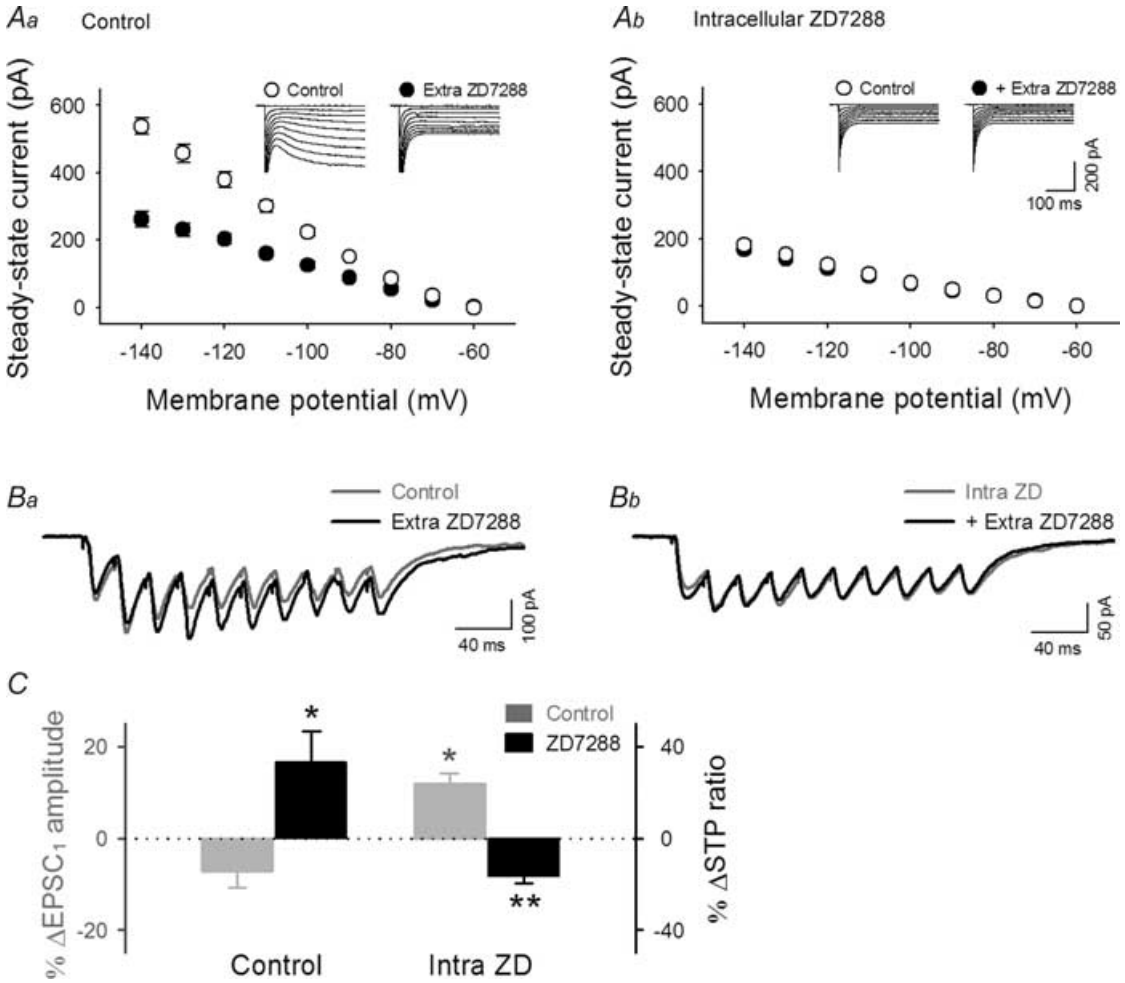

Figure 9. ZD7288 reduces STP ratios by acting on presynaptic sites, but facilitates $fEPSP_1$ by acting on postsynaptic cells

A, voltage steps from −60 mV to −70 ∼ −120 mV produced inward currents, in which the slow component, i.e. I_h current, was reduced by extracellular treatment with 30 μM ZD7288 under control conditions (*Aa*), whereas this effect was occluded when 100 μM ZD7288 was loaded into a patch pipette (*Ab*). Insets show typical raw traces. *B*, representative responses to 40-Hz trains without (*Ba*) or with intracellular ZD7288 (*Bb*) before (Control) and after extracellular treatment with 30 μM ZD7288. *A* and *B* indicate that intracellular loading of ZD7288 selectively blocks postsynaptic I_h activity. *C*, summary of the effect of extracellular ZD7288 on burst responses. $EPSC_1$ (grey) and STP ratios (black) were differentially affected by extracellular ZD7288 application. Note that the effect of extracellular ZD7288 (Extra ZD) in the presence of intracellular ZD7288 (Intra ZD) was similar to that obtained by field recordings (see Fig. 8). $^*P < 0.05$, $^{**}P < 0.01$ *versus* data without extracellular ZD7288; Tukey's test ($n = 6$ slices).

monitored the responses of the control path because ZD7288 might induce an I_h-independent rundown in synaptic transmission (Chevaleyre & Castillo, 2002), but we found no evidence for such a non-specific action, at least during our observation period (data now shown). Moreover, the effects of ZD7288 were replicated by application of 1 mM Cs^+, an inhibitor of cation channels including I_h (Fig. 8*C*). We thus conclude that the effects of ZD7288 observed here were produced by inhibition of I_h channels, not by other non-specific actions.

RSE modulates the gain of spike outputs

Most experiments above were performed in field potential recordings, so it might be important to examine whether similar RSE concurs with LTP and LTD when monitored in whole-cell patch-clamp recordings. In a voltage-clamp mode, we repeated the same procedures to compare STP in response to 40-Hz bursts before and after induction of LTP (Fig. 10*A*), LTD (Fig. 10*B*), strong LTP (Fig. 10*C*), and depotentiation (Fig. 10*D*). During application of

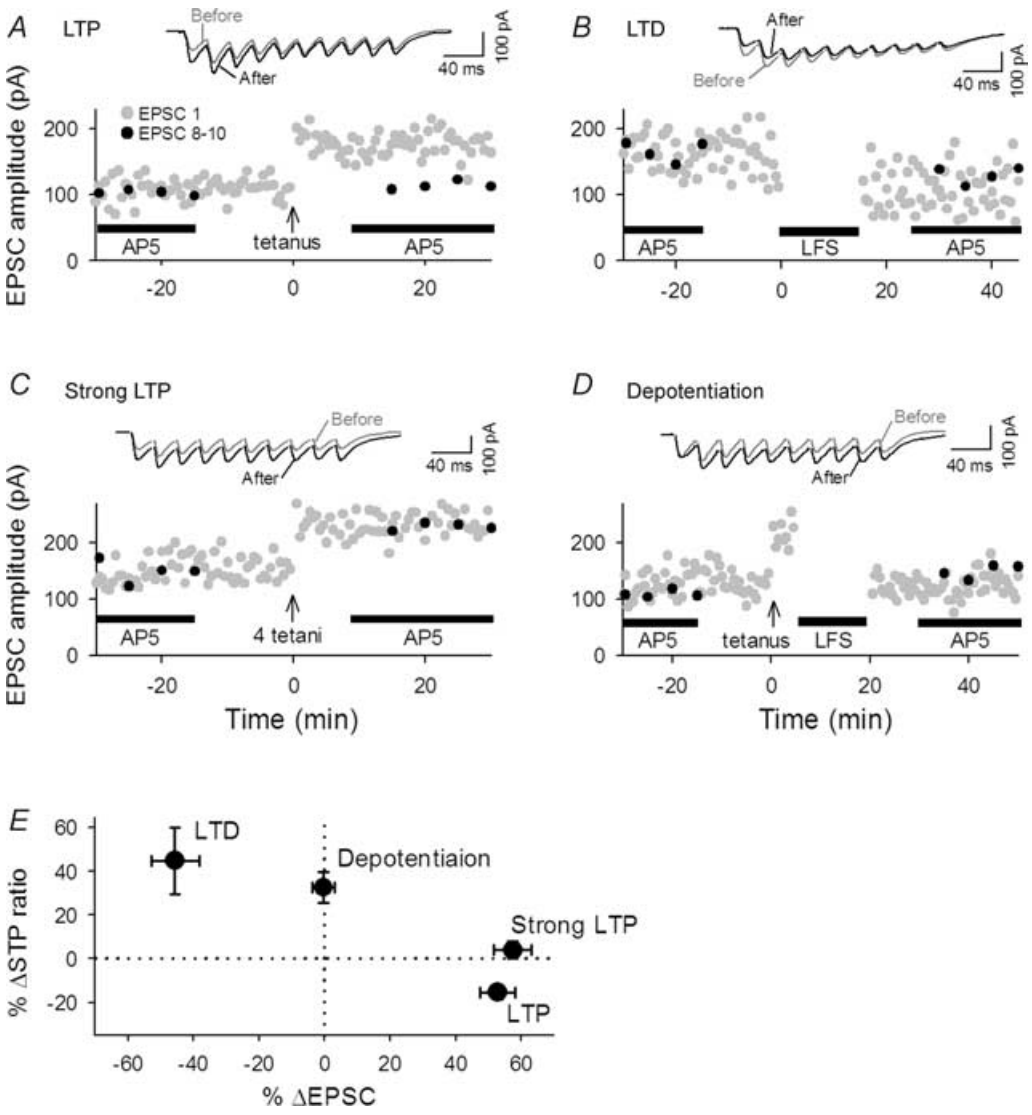

Figure 10. RSE obtained with whole-cell recordings
A–D, representative time courses in changes in EPSC sizes evoked by single-pulse test stimulation with voltage clamp at −60 mV. LTP (*A*), LTD (*B*), strong LTP (*C*), and depotentiation (*D*) were induced by a combination of current clamp of postsynaptic cells and the same stimulation of presynaptic cells as used in field potential recordings. Burst trains (40 Hz) were applied in the presence of AP5 every 5 min during time from −30 to −15 min and from 15 to 30 min. *E*, summary of data. The direction and level of plasticity and RSE were similar to those observed in field recordings (see Fig. 5). $n = 4$–7 slices.

tetanus/LFS, cells were held in a current-clamp mode without depolarizing current injection. Like Fig. 5*D*, data were summarized in Fig. 10*E*. There was no particular difference between experiments with field and patch clamp recordings.

STP is believed to affect information processing via its filtering properties (Fortune & Rose, 2001), that is, neurones use STP to transmit signals in a frequency-dependent manner. Specifically, later spikes in a burst contribute more strongly to firing of a postsynaptic neurone at facilitating synapses but less effectively at depressing synapses, as compared with the initial spike. We therefore hypothesized that RSE, i.e. a change in the profile of STP, modulates frequency-dependent transmission between neurones by changing the temporal profile of synaptic throughput. To address this possibility, CA1 pyramidal neurones were held in current clamp to monitor spiking responses to a stimulus pattern of firing activity sampled from single unit recordings of a CA3 pyramidal cell in a behaving rat (Fig. 11*A*). The natural pattern train used here was 5000 ms in length, during which 36 spikes occurred at interstimulus intervals ranging from 2.4 ms to 741.9 ms (average 116.2 ms). This template of stimulation, applied in the presence of AP5, generated characteristic firing patterns in postsynaptic cells with some variance from trial to trial.

To quantify the spike fidelity, we computed the mutual entropies between spike input from presynaptic neurones and spike output of postsynaptic neurones, which are defined as mutual information shared by both presynaptic and postsynaptic spike trains. The mutual entropies represent to what degree both activities were linked in terms of spike reliability and temporal precision. In control responses to our template stimulation, the mutual entropy was 3.01 ± 0.45 bits s^{-1} ($n = 13$ neurones) and remained stable for more than an hour (Fig. 11*D*, Control).

We examined whether the mutual entropy is changed by induction of RSE. After LTP induction (Fig. 11*Ba*), firing patterns in response to the same stimulus trains were changed (Fig. 11*Bb*), leading to an increase in mutual entropy about 3.5-fold to 10.6 ± 1.8 bits s^{-1} ($P < 0.05$) (Fig. 11*D*). This indicates that LTP enhances the temporal correlation between presynaptic inputs and postsynaptic outputs. We then applied low-frequency stimulation after triggering LTP to elicit depotentiation (Fig. 11*Ca*). Although synaptic potentials, monitored by single-pulse stimulation, returned to baseline (Fig. 11*Ca*), spiking patterns did not return to the pretetanus state (Fig. 11*Cb*). Indeed, the mutual entropy, now at 6.8 ± 1.5 bits s^{-1}, remained high after depotentiation ($P < 0.05$, $n = 6$ slices) (Fig. 11*D*).

To elucidate possible differences between potentiated and depotentiated synapses, we plotted the mutual entropy against presynaptic firing rates (Fig. 11*E*). LTP led to an increase in mutual entropy throughout the entire range of input frequencies. At depotentiated synapses, an increase in mutual entropy was preferentially observed at higher frequencies.

Discussion

Central synapses are usually weak and stochastic, and may inefficiently transmit signals by single presynaptic spikes, but burst discharges are believed to enhance the reliability of synaptic transmission (Lisman, 1997; Henze *et al.* 2002). At the same time, synapses are endowed with STP, which contributes to a fine tuning in temporal processing of burst discharges, such as frequency-selective synaptic transmission (Varela *et al.* 1997; Fortune & Rose, 2001). In this sense, long-lasting changes in the profile of STP are of importance in understanding the higher dimension of network plasticity; the significance of synaptic plasticity cannot be assessed by recording single EPSC/Ps alone. We have described the dynamics of RSE, a sign of active interactions between short-term and long-term plasticity, at hippocampal CA1 synapses, and we have shown indeed that RSE modulates spike transmission between neurones in a frequency-dependent manner. To our knowledge, this is the first evidence that the changes in STP profiles are capable of affecting synaptic performance even if the synaptic efficacy for the initial spike in burst firing is unchanged.

Many studies on LTP and LTD have focused on the change in postsynaptic functions, including changes in AMPA receptor phosphorylation and the number of functional AMPA receptors (Malinow & Malenka, 2002), but LTP is also likely to depend on alterations in presynaptic properties (Malinow & Tsien, 1990; Humeau *et al.* 2001; Zakharenko *et al.* 2003). Indeed we found that RSE has a presynaptic origin. Several studies have addressed presynaptic changes after LTP induction, but most have focused on synaptic responses to paired-pulse stimuli and have sometimes led to inconsistent conclusions (Clark *et al.* 1994; Kuhnt & Voronin, 1994; Schulz *et al.* 1994; Wang & Kelly, 1996). Paired-pulse analyses cannot evaluate presynaptic properties comprehensively; paired-pulse stimuli can only reveal one of the transitional phases of STP. Moreover, paired-pulse synaptic responses are modified by further preceding synaptic inputs, and therefore, experiments using three or more repetitive stimuli are essential in understanding the profile of STP. In this respect, our approaches using burst trains and natural patterns of stimuli could reveal the basic features of STP.

RSE was induced by activation of NMDA receptors whereas its expression is presynaptic. Although the mechanisms linking NMDA receptor activity to presynaptic expression of RSE cannot be deduced from the present study alone, there could be at least two different, but not mutually exclusive, explanations. First,

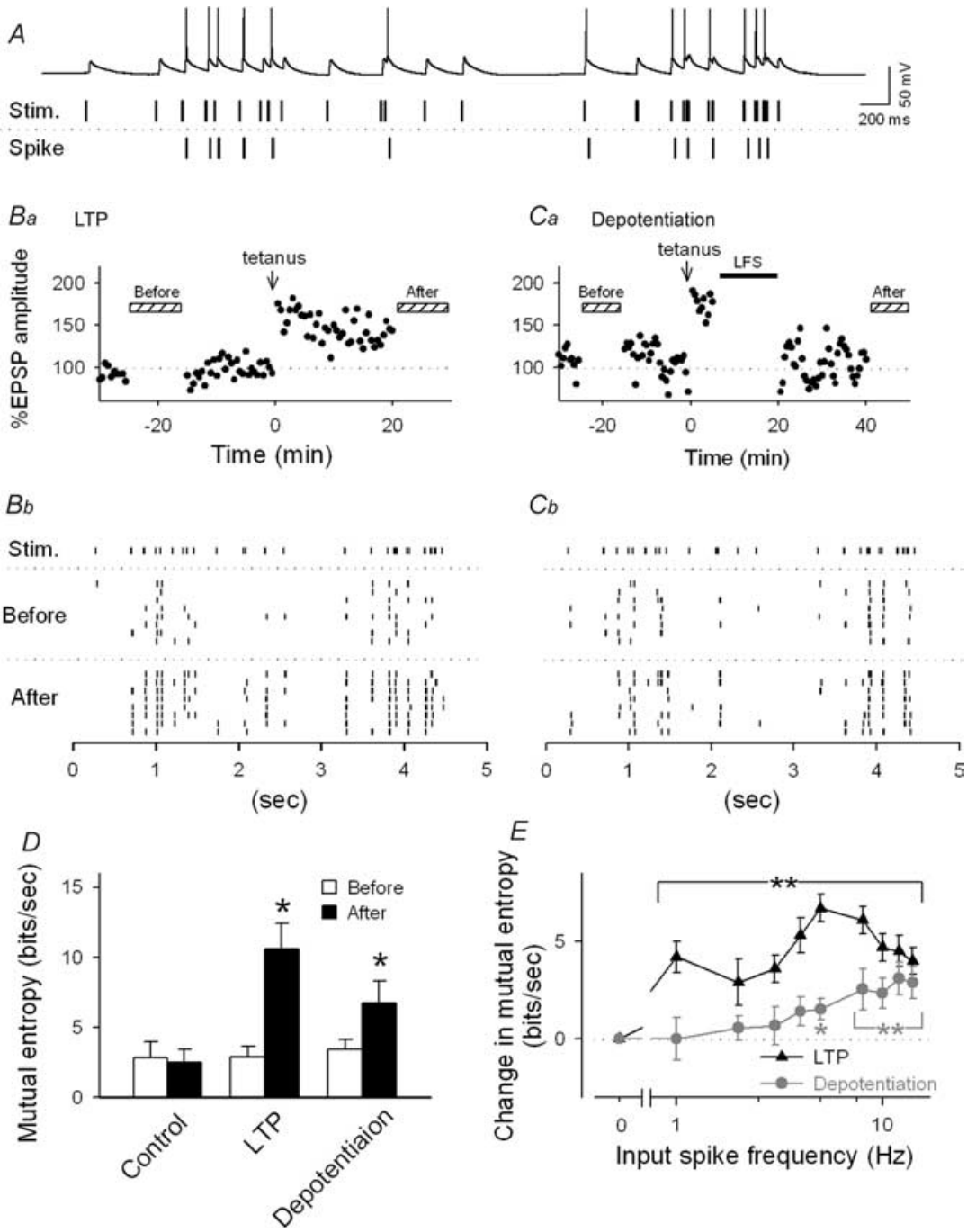

Figure 11. RSE modifies a frequency preference in spike responses
A, upper trace: typical spiking activity generated by a CA1 pyramidal cell in response to a stimulus train with a natural temporal pattern (middle trace) sampled from a CA3 pyramidal cell in a free-moving rat. Bottom trace: extracted spikes. *B*–*C*, representative firing responses 20 min before and 30 min after induction of LTP (*B*) or depotentiation (*C*). *Ba* and *Ca* show the time courses of changes in EPSP1 evoked by single-pulse test stimulation in a current clamp mode. Rasterplots (*Bb* and *Cb*) show timings of spikes evoked by the same natural stimulus trains. The trains were applied 8 times every 60–120 s during the periods indicated by the hatched bars in the panels *Ba* and *Ca*. *D*, quantification of information transmitted from presynaptic to postsynaptic sites before and after induction of LTP and depotentiation. Mutual entropy enhanced by LTP was retained after depotentiation. *E*, frequency-dependent information transmission. At depotentiated synapses, the mutual entropy was increased in a frequency-specific manner (grey) whereas synapses with LTP displayed a broad increase (black). $^{*}P < 0.05$, $^{**}P < 0.01$ *versus* basal response; Tukey's test ($n = 3$–6 slices).

postsynaptic NMDA receptors may recruit retrograde signalling from postsynaptic sites to presynaptic terminals. At neocortical layer 5 pyramidal cells, endocannabinoids have recently been implicated as retrograde molecules that may trigger RSE (Sjostrom *et al.* 2003). Second, NMDA receptors at presynaptic sites may directly trigger RSE. Presynaptic NMDA receptors have recently been suggested to contribute to synaptic plasticity (Siegel *et al.* 1994; Berretta & Jones, 1996; MacDermott *et al.* 1999; Humeau *et al.* 2003; Sjostrom *et al.* 2003). At present, however, there is no compelling evidence for the existence of presynaptic NMDA receptors in the CA1 region.

In contrast to the case of RSE induction, nothing was known about the molecular basis of RSE maintenance. We have shown that RSE is expressed, at least in part, through a change in presynaptic I_h activity. I_h channel activity is known to be a key component in rhythmic neuronal activity, dendritic integration and membrane excitability (Robinson & Siegelbaum, 2003; Soleng *et al.* 2003, 2004), but its role in shaping STP has not been reported. Our findings therefore provide a new function of I_h channels. Consistent with a previous report (Chevaleyre & Castillo, 2002), ZD7288 and Cs^+ elicited a slight augmentation of initial synaptic transmission, i.e. an increase in $fEPSP_1$, which indicates that I_h channels are constitutively active under basal conditions. At the same time, ZD7288 and Cs^+ also induced a substantial reduction in the STP ratio under basal conditions, which indicates that I_h activity shifts the profile of STP toward facilitation, thereby opposing synaptic depression at CA1 synapses. By analogy with the role of I_h in dendritic integration (Magee, 1998, 1999; and see also Fig. 8*Ba*), we consider that I_h channels contribute to temporal integration of axonal signals. Because I_h channels have cationic conductances with slow activation, I_h may facilitate burst-induced Ca^{2+} accumulation at synaptic terminals and increase release probability. In this respect, it is intriguing that LTP abolished the inhibitory effect of ZD7288 on STP without affecting the facilitatory effect on $fEPSP_1$. LTP-induced RSE is presumably due to a decline of constitutive I_h activity.

LTP induced by strong tetanus was not accompanied by RSE, however. Strong tetanus often recruits the 'late phase' of LTP (Frey *et al.* 1988; Huang *et al.* 1996; Bolshakov *et al.* 1997), which involves the formation of new sites of synaptic transmission (Bolshakov *et al.* 1997). Such new synapses may have a low probability of neurotransmitter release and display the naive property of STP. As a result, the level of STP after strong tetanus could be similar to pretetanic baseline. However, this is unlikely to be the case, especially because RSE can take place within a few minutes after tetanus, and this time scale is too short for synaptogenesis. Moreover, RSE induced by strong tetanus was unmasked by pharmacological blockade of $GABA_B$ receptors.

There are two possibilities that could explain the contribution of $GABA_B$ receptors. First, $GABA_B$ receptor activation prevents the induction mechanisms of RSE. $GABA_B$ receptor activation decreases intracellular cAMP levels, which may inhibit long-lasting modulation of I_h activity. The second possibility is that the level of $GABA_B$ receptor activity is persistently enhanced and masks LTP-induced RSE. Such persistent activation of $GABA_B$ receptors could be brought about by LTP at inhibitory synapses of interneurones, and these inhibitory inputs are usually polysynaptic, so the RSE masking may occur only when a strong tetanus is presented.

Several studies reported that unlike neocortical synapses, hippocampal synapses do not display RSE (Pananceau *et al.* 1998; Selig *et al.* 1999; Buonomano, 1999), but we have shown that hippocampal synapses are capable of showing RSE. This apparent inconsistency could be due to different experimental protocols for plasticity induction. Specifically, membrane depolarization or current injection into postsynaptic cells during plasticity induction may recruit different mechanisms of synaptic plasticity; we did not apply such artificial stimulation to postsynaptic cells but instead we current-clamped them during presynaptic stimulation. Nonetheless, importantly, we found that at hippocampal synapses, both LTP with and LTP without RSE were induced by the same experimental protocol, except just for the 'intensity' of tetanic stimulation. We thus consider that RSE is perhaps prevalent at cortical excitatory synapses, but that the induction of RSE requires a specific pattern of presynaptic activation.

With dynamic properties of RSE, the synapses are assigned a wider range of complexity than expected hitherto. The finding that, depending on the input intensity, they are capable of exhibiting different degrees of STP with the same extent of changes in the initial EPSPs is of particular importance because the presence or absence of RSE has different effects on information processing. At potentiated synapses without RSE (i.e. unchanged STP ratio), information is evenly amplified, i.e. a general 'gain' increase in signals conveyed between neurones, whereas LTP with RSE transforms the 'content' of the signals. The present study has shown that by modifying RSE, LTP can shift between these distinct processing modes and suggests that LTP is not a single-dimension phenomenon, but can rather have multifaceted functions that cannot be estimated by monitoring single EPSPs alone, as has been done in most previous studies.

Neural messages are ultimately conveyed by action potentials. With natural patterns of presynaptic activity, RSE was seen to modulate the spiking behaviour. To our knowledge, the present work is the first attempt to assess synaptic plasticity using information theory, showing that LTP enhances the mutual entropy of information transmission. Even at depotentiated synapses, RSE remained, gating the flow of signals, in which case the signals had a more specific frequency band

to transmit synaptic inputs, as compared to synapses with LTP. Depotentiation/dedepression, hence, is not an 'undoing' of LTP/LTD but rather represents another level of plasticity and can store information about how the synapses have experienced plastic modulation in the past. We thus conclude that RSE represents 'synaptic states' and serves as a historic record of synaptic plasticity. This predicts a novel syntax of circuit operations, i.e. state-dependent propagations of neural signals. Elucidating RSE would reveal the computational significance of synaptic modifications.

References

Abbott LF & Nelson SB (2000). Synaptic plasticity: taming the beast. *Nat Neurosci* **3** (Suppl.), 1178–1183.

Abbott LF, Varela JA, Sen K & Nelson SB (1997). Synaptic depression and cortical gain control. *Science* **275**, 220–224.

Abi-Gerges N, Ji GJ, Lu ZJ, Fischmeister R, Hescheler J & Fleischmann BK (2000). Functional expression and regulation of the hyperpolarization activated non-selective cation current in embryonic stem cell-derived cardiomyocytes. *J Physiol* **523**, 377–389.

Berretta N & Jones RS (1996). Tonic facilitation of glutamate release by presynaptic N-methyl-D-aspartate autoreceptors in the entorhinal cortex. *Neuroscience* **75**, 339–344.

Bienenstock EL, Cooper LN & Munro PW (1982). Theory for the development of neuron selectivity: orientation specificity and binocular interaction in visual cortex. *J Neurosci* **2**, 32–48.

Bliss TV & Collingridge GL (1993). A synaptic model of memory: long-term potentiation in the hippocampus. *Nature* **361**, 31–39.

Bolshakov VY, Golan H, Kandel ER & Siegelbaum SA (1997). Recruitment of new sites of synaptic transmission during the cAMP-dependent late phase of LTP at CA3-CA1 synapses in the hippocampus. *Neuron* **19**, 635–651.

Brenowitz S, David J & Trussell L (1998). Enhancement of synaptic efficacy by presynaptic $GABA_B$ receptors. *Neuron* **20**, 135–141.

Buonomano DV (1999). Distinct functional types of associative long-term potentiation in neocortical and hippocampal pyramidal neurons. *J Neurosci* **19**, 6748–6754.

Buonomano DV & Merzenich MM (1995). Temporal information transformed into a spatial code by a neural network with realistic properties. *Science* **267**, 1028–1030.

Caillard O, Ben Ari Y & Gaiarsa JL (1999). Long-term potentiation of GABAergic synaptic transmission in neonatal rat hippocampus. *J Physiol* **518**, 109–119.

Chevaleyre V & Castillo PE (2002). Assessing the role of Ih channels in synaptic transmission and mossy fiber LTP. *Proc Natl Acad Sci U S A* **99**, 9538–9543.

Clark KA, Randall AD & Collingridge GL (1994). A comparison of paired-pulsed facilitation of AMPA and NMDA receptor-mediated excitatory postsynaptic currents in the hippocampus. *Exp Brain Res* **101**, 272–278.

Cook DL, Schwindt PC, Grande LA & Spain WJ (2003). Synaptic depression in the localization of sound. *Nature* **421**, 66–70.

Csicsvari J, Lamieson B, Wise KD & Buzsaki G (2003). Mechanisms of gamma oscillations in the hippocampus of the behaving rat. *Neuron* **37**, 311–322.

Dittman JS, Kreitzer AC & Regehr WG (2000). Interplay between facilitation, depression, and residual calcium at three presynaptic terminals. *J Neurosci* **20**, 1374–1385.

Dobrunz LE & Stevens CF (1997). Heterogeneity of release probability, facilitation, and depletion at central synapses. *Neuron* **18**, 995–1008.

Dobrunz LE & Stevens CF (1999). Response of hippocampal synapses to natural stimulation patterns. *Neuron* **22**, 157–166.

Dudek SM & Bear MF (1993). Bidirectional long-term modification of synaptic effectiveness in the adult and immature hippocampus. *J Neurosci* **13**, 2910–2918.

Fortune ES & Rose GJ (2001). Short-term synaptic plasticity as a temporal filter. *Trends Neurosci* **24**, 381–385.

Frey U, Krug M, Reymann KG & Matthies H (1988). Anisomycin, an inhibitor of protein synthesis, blocks late phases of LTP phenomena in the hippocampal CA1 region in vitro. *Brain Res* **452**, 57–65.

Fujii S, Saito K, Miyakawa H, Ito K & Kato H (1991). Reversal of long-term potentiation (depotentiation) induced by tetanus stimulation of the input to CA1 neurons of guinea pig hippocampal slices. *Brain Res* **555**, 112–122.

Gerber U & Gahwiler BH (1994). $GABA_B$ and adenosine receptors mediate enhancement of the K^+ current, I_{AHP}, by reducing adenylyl cyclase activity in rat CA3 hippocampal neurons. *J Neurophysiol* **72**, 2360–2367.

Harris NC & Constanti A (1995). Mechanism of block by ZD 7288 of the hyperpolarization-activated inward rectifying current in guinea pig substantia nigra neurons in vitro. *J Neurophysiol* **74**, 2366–2378.

Henze DA, Wittner L & Buzsaki G (2002). Single granule cells reliably discharge targets in the hippocampal CA3 network in vivo. *Nat Neurosci* **5**, 790–795.

Huang CC, Liang YC & Hsu KS (2001). Characterization of the mechanism underlying the reversal of long term potentiation by low frequency stimulation at hippocampal CA1 synapses. *J Biol Chem* **276**, 48108–48117.

Huang YY, Nguyen PV, Abel T & Kandel ER (1996). Long-lasting forms of synaptic potentiation in the mammalian hippocampus. *Learn Mem* **3**, 74–85.

Humeau Y, Shaban H, Bissiere S & Luthi A (2003). Presynaptic induction of heterosynaptic associative plasticity in the mammalian brain. *Nature* **426**, 841–845.

Kuhnt U & Voronin LL (1994). Interaction between paired-pulse facilitation and long-term potentiation in area CA1 of guinea-pig hippocampal slices: application of quantal analysis. *Neuroscience* **62**, 391–397.

Lee HK, Barbarosie M, Kameyama K, Bear MF & Huganir RL (2000). Regulation of distinct AMPA receptor phosphorylation sites during bidirectional synaptic plasticity. *Nature* **405**, 955–959.

Lisman JE (1997). Bursts as a unit of neural information: making unreliable synapses reliable. *Trends Neurosci* **20**, 38–43.

London M, Schreibman A, Hausser M, Larkum ME & Segev I (2002). The information efficacy of a synapse. *Nat Neurosci* **5**, 332–340.

Lu KT & Gean PW (1999). Masking of forskolin-induced long-term potentiation by adenosine accumulation in area CA1 of the rat hippocampus. *Neuroscience* **88**, 69–78.
MacDermott AB, Role LW & Siegelbaum SA (1999). Presynaptic ionotropic receptors and the control of transmitter release. *Annu Rev Neurosci* **22**, 443–485.
Magee JC (1998). Dendritic hyperpolarization-activated currents modify the integrative properties of hippocampal CA1 pyramidal neurons. *J Neurosci* **18**, 7613–7624.
Magee JC (1999). Dendritic I_h normalizes temporal summation in hippocampal CA1 neurons. *Nat Neurosci* **2**, 508–514.
Malinow R & Malenka RC (2002). AMPA receptor trafficking and synaptic plasticity. *Annu Rev Neurosci* **25**, 103–126.
Malinow R & Tsien RW (1990). Presynaptic enhancement shown by whole-cell recordings of long-term potentiation in hippocampal slices. *Nature* **46**, 177–180.
Markram H & Tsodyks M (1996*a*). Redistribution of synaptic efficacy between neocortical pyramidal neurons. *Nature* **382**, 807–810.
Markram H & Tsodyks M (1996*b*). Redistribution of synaptic efficacy: a mechanism to generate infinite synaptic input diversity from a homogeneous population of neurons without changing absolute synaptic efficacies. *J Physiol Paris* **90**, 229–232.
Mellor J, Nicoll RA & Schmitz D (2002). Mediation of hippocampal mossy fiber long-term potentiation by presynaptic I_h channels. *Science* **295**, 143–147.
Misgeld U, Bijak M & Jarolimek W (1995). A physiological role for $GABA_B$ receptors and the effects of baclofen in the mammalian central nervous system. *Prog Neurobiol* **46**, 423–462.
Pananceau M, Chen H & Gustafsson B (1998). Short-term facilitation evoked during brief afferent tetani is not altered by long-term potentiation in the guinea-pig hippocampal CA1 region. *J Physiol* **508**, 503–514.
Pape HC (1996). Queer current and pacemaker: the hyperpolarization-activated cation current in neurons. *Annu Rev Physiol* **58**, 299–327.
Perez Y, Chapman CA, Woodhall G, Robitaille R & Lacaille JC (1999). Differential induction of long-lasting potentiation of inhibitory postsynaptic potentials by theta patterned stimulation versus 100-Hz tetanization in hippocampal pyramidal cells in vitro. *Neuroscience* **90**, 747–757.
Rieke F, Warland D, de Ruyter van Steveninck R & Bialek W (1997). *Spikes: Exploring the Neural Code*. MIT Press, Cambridge, MA, USA.
Robinson RB & Siegelbaum SA (2003). Hyperpolarization-activated cation currents: from molecules to physiological function. *Annu Rev Physiol* **65**, 453–480.
Santoro B, Chen S, Luthi A, Pavlidis P, Shumyatsky GP, Tibbs GR & Siegelbaum SA (2000). Molecular and functional heterogeneity of hyperpolarization-activated pacemaker channels in the mouse CNS. *J Neurosci* **20**, 5264–5275.
Schulz PE, Cook EP & Johnston D (1994). Changes in paired-pulse facilitation suggest presynaptic involvement in long-term potentiation. *J Neurosci* **14**, 5325–5337.
Selig DK, Nicoll RA & Malenka RC (1999). Hippocampal long-term potentiation preserves the fidelity of postsynaptic responses to presynaptic bursts. *J Neurosci* **19**, 1236–1246.
Siegel SJ, Brose N, Janssen WG, Gasic GP, Jahn R, Heinemann SF & Morrison JH (1994). Regional, cellular, and ultrastructural distribution of N-methyl-D-aspartate receptor subunit 1 in monkey hippocampus. *Proc Natl Acad Sci U S A* **91**, 564–568.
Sjostrom PJ, Turrigiano GG & Nelson SB (2003). Neocortical LTD via coincident activation of presynaptic NMDA and cannabinoid receptors. *Neuron* **39**, 641–654.
Soleng AF, Baginskas A, Anderson P & Raastad M (2004). Activity-dependent excitability changes in hippocampal CA3 cell Schaffer axons. *J Physiol* **560**, 491–503.
Soleng AF, Chiu K & Raastad M (2003). Unmyelinated axons in the rat hippocampus hyperpolarize and activate an H current when spike frequency exceeds 1 Hz. *J Physiol* **552**, 459–470.
Southan AP, Morris NP, Stephens GJ & Robertson B (2000). Hyperpolarization-activated currents in presynaptic terminals of mouse cerebellar basket cells. *J Physiol* **526**, 91–97.
Staubli U & Scafidi J (1999). Time-dependent reversal of long-term potentiation in area CA1 of the freely moving rat induced by theta pulse stimulation. *J Neurosci* **19**, 8712–8719.
Tanaka T, Saito H & Matsuki N (1997). Inhibition of $GABA_A$ synaptic responses by brain-derived neurotrophic factor (BDNF) in rat hippocampus. *J Neurosci* **17**, 2959–2966.
Tsodyks MV & Markram H (1997). The neural code between neocortical pyramidal neurons depends on neurotransmitter release probability. *Proc Natl Acad Sci U S A* **94**, 719–723.
Ueno S, Tsukamoto M, Hirano T, Kikuchi K, Yamada MK, Nishiyama N, Nagano T, Matsuki N & Ikegaya Y (2002). Mossy fiber Zn^{2+} spillover modulates heterosynaptic *N*-methyl-D-aspartate receptor activity in hippocampal CA3 circuits. *J Cell Biol* **158**, 215–220.
Varela JA, Sen K, Gibson J, Fost J, Abbott LF & Nelson SB (1997). A quantitative description of short-term plasticity at excitatory synapses in layer 2/3 of rat primary visual cortex. *J Neurosci* **17**, 7926–7940.
Wang JH & Kelly PT (1996). Regulation of synaptic facilitation by postsynaptic Ca^{2+}/CaM pathways in hippocampal CA1 neurons. *J Neurophysiol* **76**, 276–286.
Zakharenko SS, Zablow L & Siegelbaum SA (2001). Visualization of changes in presynaptic function during long-term synaptic plasticity. *Nat Neurosci* **4**, 711–717.
Zucker RS & Regehr WG (2002). Short-term synaptic plasticity. *Annu Rev Physiol* **64**, 355–405.

Acknowledgements

We would like to thank Dr Yoshio Sakurai (Kyoto University) for generously providing us with *in vivo* spike timing patterns. We are grateful to Dr Cynthia Lang (Siegelbaum lab, Columbia University) for helpful discussions and comments on an early version of the manuscript.

Dynamic synapses as archives of synaptic history: state-dependent redistribution of synaptic efficacy in the rat hippocampal CA1

Takuya Yasui, Shigeyoshi Fujisawa, Masako Tsukamoto, Norio Matsuki and Yuji Ikegaya

J. Physiol. 2005;566;143-160; originally published online Apr 21, 2005;

DOI: 10.1113/jphysiol.2005.086595